Nonlinear Stretching Flow with Thermal Radiation

Tasawar Hayat[a,b], Rabia Noureen[a], and Tariq Javed[c]

[a] Department of Mathematics, Quaid-I-Azam University 45320, Islamabad 44000, Pakistan
[b] Department of Mathematics, College of Sciences, King Saud University, P. O. Box 2455, Riyadh 11451, Saudi Arabia
[c] Faculty of Basic and Applied Sciences, International Islamic University, Islamabad 44000, Pakistan

Reprint requests to T. H.; Fax: +92 51 2601171. E-mail: pensy_t@yahoo.com

Z. Naturforsch. **65a,** 761 – 770 (2010); received May 4, 2009

This work concerns with the radiation effects on rotating boundary layer flow of an electrically conducting incompressible fluid over a nonlinear stretching surface. The viscous fluid fills the porous space. The flow is permeated by a constant magnetic field applied in the transverse direction. Two types of temperatures are prescribed to the surface. The resulting problems of velocity and temperature are obtained using the homotopy analysis method (HAM). Convergence of the developed series solutions is carefully checked. Graphical results of the velocity and temperature fields for various values of the parameters of the problems are presented and discussed.

Key words: Nonlinear Stretching; Radiation Effect; Porous Space; Series Solutions.

1. Introduction

Nonlinear equations play an important role in the study of physical phenomena. In general, the problems in fluid mechanics are nonlinear. In most cases it is difficult to solve such nonlinear problems not only analytically but numerically also. However, the analytic solutions of the nonlinear flow problems are rare even under the simplified assumptions. Therefore the construction of an analytic solution to a nonlinear problem is an important task. Currently, the homotopy analysis method (HAM) introduced by Liao [1, 2] is regarded an effective tool for the analytic solutions. This method has been successfully applied to many nonlinear problems [3 – 20]. All these studies verified the validity and flexibility of HAM. It is noticed that HAM does not depend upon any small or large parameter.

It is well known that radiative magnetohydrodynamic (MHD) flows arise in electrical power generation, astrophysical flows, solar power technology, and other engineering and industrial applications [21, 22]. Motivated by such facts, Raptis et al. [23] studied the effect of thermal radiation on the flow of a viscous fluid past a semi-infinite plate. In continuation, the purpose of the present investigation is to study the influence of thermal radiation on MHD rotating flow over a nonlinear stretching surface. An incompressible viscous fluid fills the porous space. The nonlinear flow problem is formulated. Two sets of boundary conditions regarding the temperature are imposed. Series solutions of velocity and temperature distributions are constructed. Graphs are displayed and analyzed for the various parameters of interest.

2. Mathematical Formulation

Consider the steady flow of a MHD viscous fluid with heat transfer past a flat surface. The surface at $z = 0$ is stretched nonlinearly in x-direction. Both fluid and surface are rotating with constant angular velocity $\boldsymbol{\Omega}$ about the z-axis taken normal to the surface. A uniform magnetic field is applied in the z-direction. This gives rise to magnetic effects in x- and z-directions. Heat transfer analysis is taken into account and all fluid properties are chosen constant. The magnetic Reynolds number is assumed small and the induced magnetic field is neglected. Under the aforementioned assumptions the equations governing the flow are

$$\frac{\partial u}{\partial x}+\frac{\partial v}{\partial y}+\frac{\partial w}{\partial z}=0, \tag{1}$$

$$\left(u\frac{\partial}{\partial x}+v\frac{\partial}{\partial y}+w\frac{\partial}{\partial z}\right)u-2\Omega v=-\frac{1}{\rho}\frac{\partial p}{\partial x} +\nu\left(\frac{\partial^2}{\partial x^2}+\frac{\partial^2}{\partial y^2}+\frac{\partial^2}{\partial z^2}\right)u-\frac{\sigma B_0^2}{\rho}u-\frac{\phi\nu}{k}u, \tag{2}$$

0932–0784 / 10 / 1000–0761 $ 06.00

$$\left(u\frac{\partial}{\partial x}+v\frac{\partial}{\partial y}+w\frac{\partial}{\partial z}\right)v+2\Omega u=-\frac{1}{\rho}\frac{\partial p}{\partial y}+\nu\left(\frac{\partial^2}{\partial x^2}+\frac{\partial^2}{\partial y^2}+\frac{\partial^2}{\partial z^2}\right)v-\frac{\sigma B_0^2}{\rho}v-\frac{\phi\nu}{k}v, \tag{3}$$

$$\left(u\frac{\partial}{\partial x}+v\frac{\partial}{\partial y}+w\frac{\partial}{\partial z}\right)w=-\frac{1}{\rho}\frac{\partial p}{\partial z}+\nu\left(\frac{\partial^2}{\partial x^2}+\frac{\partial^2}{\partial y^2}+\frac{\partial^2}{\partial z^2}\right)w-\frac{\phi\nu}{k}w, \tag{4}$$

$$\rho c_{\mathrm{p}}\left(u\frac{\partial}{\partial x}+v\frac{\partial}{\partial y}+w\frac{\partial}{\partial z}\right)T=k_1\left(\frac{\partial^2}{\partial x^2}+\frac{\partial^2}{\partial y^2}+\frac{\partial^2}{\partial z^2}\right)T+\Phi-\left(\frac{\partial}{\partial x}+\frac{\partial}{\partial y}+\frac{\partial}{\partial z}\right)q_{\mathrm{r}}. \tag{5}$$

In above equations u, v, and w are the velocity components in x, y, and z-directions, σ is the electrical conductivity, ν $(=\frac{\mu}{\rho})$ is the kinematic viscosity, μ is the dynamic viscosity, ρ is the density, p is the modified pressure including the centrifugal force term, ϕ is the porosity, k is the permeability of the porous medium, c_{p} is the specific heat, T is the temperature, k_1 is the thermal conductivity of the fluid, and q_{r} is the radiative heat flux.

The dissipation function Φ is

$$\Phi=2\mu\left[\left(\frac{\partial u}{\partial x}\right)^2+\left(\frac{\partial v}{\partial y}\right)^2+\left(\frac{\partial w}{\partial z}\right)^2+\frac{1}{2}\left(\frac{\partial v}{\partial x}+\frac{\partial u}{\partial y}\right)^2+\frac{1}{2}\left(\frac{\partial w}{\partial y}+\frac{\partial v}{\partial z}\right)^2+\frac{1}{2}\left(\frac{\partial u}{\partial z}+\frac{\partial w}{\partial x}\right)^2\right]. \tag{6}$$

By Rosseland approximation of radiation for an optically thick layer one may write

$$q_{\mathrm{r}}=-\frac{4\sigma^*}{3k^*}\frac{\partial T^4}{\partial z}, \tag{7}$$

where σ^* is the Stefan-Boltzmann constant and k^* is the mean absorption coefficient. We express the term T^4 as a linear function of temperature in a Taylor series about T_∞ and neglect higher terms, therefore we have

$$T^4\cong 4T_\infty^3T-3T_\infty^4. \tag{8}$$

The boundary conditions suggested by the physics of the problem are

$$\begin{aligned}&u=u_{\mathrm{w}}=cx^n,\quad v=0,\quad w=0\ \text{ at }\ z=0,\\&u\to 0,\quad v\to 0\ \text{ as }\ z\to\infty,\end{aligned} \tag{9}$$

in which c and n are the parameters related to the speed of the stretching surface.

For the temperature we have the following two sets of boundary conditions:

Case a: Constant surface temperature (*CST*)

$$\begin{aligned}&T=T_{\mathrm{w}}\quad \text{at }\ z=0,\\&T\to T_\infty\quad \text{as }\ z\to\infty.\end{aligned} \tag{10}$$

Case b: Prescribed surface temperature (*PST*)

$$\begin{aligned}&T=T_{\mathrm{w}}(=T_\infty+Ax^K)\quad \text{at }\ z=0,\\&T\to T_\infty\qquad\qquad\quad \text{as }\ z\to\infty,\end{aligned} \tag{11}$$

where K is the surface temperature parameter.

By using the transformations

$$\begin{aligned}&u=cx^nf'(\eta),\quad v=cx^ng(\eta),\\&\eta=\sqrt{\frac{c(n+1)}{2\nu}}x^{\frac{n-1}{2}}z,\\&w=-\sqrt{\frac{c\nu(n+1)}{2}}x^{\frac{n-1}{2}}\left[f(\eta)+\frac{n-1}{n+1}\eta f'(\eta)\right],\\&\theta(\eta)=\frac{T-T_\infty}{T_{\mathrm{w}}-T_\infty}\end{aligned} \tag{12}$$

the continuity equation (1) is identically satisfied and (2)–(4) and (9) give

$$f'''(\eta)-\frac{2n}{n+1}f'^2(\eta)+f(\eta)f''(\eta)+\frac{4\lambda}{n+1}g(\eta)-M^2f'(\eta)-\phi f'(\eta)=0, \tag{13}$$

$$g''(\eta)-\frac{2n}{n+1}g(\eta)f'(\eta)+g'(\eta)f(\eta)-\frac{4\lambda}{n+1}f'(\eta)-M^2g(\eta)-\phi g(\eta)=0, \tag{14}$$

$$f(0)=0,\quad f'(0)=1,\quad g(0)=0, \tag{15}$$

$$f'\to 0,\ g\to 0\ \text{ as }\ \eta\to\infty, \tag{16}$$

where

$$M^2=\frac{2\sigma B_0^2}{c\rho(n+1)x^{n-1}},\quad \lambda=\frac{\Omega}{cx^{n-1}},\quad \phi=\frac{2\nu\phi}{ck(n+1)x^{n-1}}. \tag{17}$$

The shear stresses at the surface in x and y-directions are

$$\tau_{xz} = c\mu\sqrt{\frac{c(n+1)}{2\nu}}x^{\frac{3n-1}{2}}f''(0), \tag{18}$$

$$\tau_{yz} = c\mu\sqrt{\frac{c(n+1)}{2\nu}}x^{\frac{3n-1}{2}}g'(0). \tag{19}$$

Now (5), (10), and (11) lead to the following problems of temperature:

Case a: Constant surface temperature (*CST*)

$$\begin{aligned}&(3R_{\mathrm{d}}+4)\theta''(\eta)+3\,\mathrm{Pr}R_{\mathrm{d}}\Big[\theta'(\eta)f(\eta)\\&+\mathrm{Ec}\{f''^2(\eta)+g'^2(\eta)\}\Big]=0,\end{aligned} \tag{20}$$

$$\theta(0)=1, \quad \theta(\infty)\to 0, \tag{21}$$

and the rate of heat transfer is

$$-\lambda_{\mathrm{T}}\left(\frac{\mathrm{d}T}{\mathrm{d}z}\right) = -\lambda_{\mathrm{T}}(T_{\mathrm{w}}-T_{\infty})\theta'(0)\sqrt{\frac{c(n+1)}{2\nu}}x^{\frac{n-1}{2}}. \tag{22}$$

Case b: Prescribed surface temperature (*PST*)

$$\begin{aligned}&(3R_{\mathrm{d}}+4)\theta''(\eta)+3R_{\mathrm{d}}\,\mathrm{Pr}\,\theta'(\eta)f(\eta)\\&-3R_{\mathrm{d}}\,\mathrm{Pr}\frac{2K}{n+1}f'(\eta)\theta(\eta)=\\&-3R_{\mathrm{d}}\,\mathrm{Pr}\,\tilde{\mathrm{E}}\mathrm{c}\,x^{2n-K}(f''^2(\eta)+g'^2(\eta)).\end{aligned} \tag{23}$$

The above equation for $K=2n$ reduces to

$$\begin{aligned}&(3R_{\mathrm{d}}+4)\theta''(\eta)+3R_{\mathrm{d}}\,\mathrm{Pr}\,\theta'(\eta)f(\eta)\\&-3R_{\mathrm{d}}\,\mathrm{Pr}\frac{4n}{n+1}f'(\eta)\theta(\eta)=\\&-3R_{\mathrm{d}}\,\mathrm{Pr}\,\tilde{\mathrm{E}}\mathrm{c}(f''^2(\eta)+g'^2(\eta)),\end{aligned} \tag{24}$$

$$\theta(0)=1, \quad \theta(\infty)\to 0. \tag{25}$$

The local surface heat flux is

$$\begin{aligned}q_{\mathrm{w}} &= -\lambda_{\mathrm{T}}\left(\frac{\mathrm{d}T}{\mathrm{d}z}\right)\\&= -\lambda_{\mathrm{T}}Ax^{\frac{2K+n-1}{2}}\theta'(0)\sqrt{\frac{c(n+1)}{2\nu}}.\end{aligned} \tag{26}$$

Here the Prandtl number Pr, the radiation parameter R_{d}, the Eckert numbers Ec and $\tilde{\mathrm{E}}\mathrm{c}$ are given by

$$\begin{aligned}&\mathrm{Pr}=\frac{\mu c_{\mathrm{p}}}{k_1}, \quad R_{\mathrm{d}}=\frac{k^*k_1}{4\sigma^*T_\infty^3},\\&\mathrm{Ec}=\frac{u_{\mathrm{w}}^2}{c_{\mathrm{p}}(T_{\mathrm{w}}-T_\infty)}, \quad \tilde{\mathrm{E}}\mathrm{c}=\frac{c^2}{Ac_{\mathrm{p}}}.\end{aligned} \tag{27}$$

The analytical solutions of the governing nonlinear problems consisting of (13)–(16) and (20), (21), (24), and (25) will be presented in the next section by employing a homotopy analysis method (HAM).

3. Analytical Solution of Velocity f(η)

For HAM solutions we select the initial approximations

$$f_0(\eta)=1-\exp(-\eta), \quad g_0(\eta)=\eta\exp(-\eta) \tag{28}$$

and the auxiliary linear operators

$$\mathcal{L}_{\mathrm{f}}=f'''-f', \quad \mathcal{L}_{\mathrm{g}}=g''-g, \tag{29}$$

$$\begin{aligned}&\mathcal{L}_{\mathrm{f}}(C_1\mathrm{e}^{\eta}+C_2+C_3\mathrm{e}^{-\eta})=0,\\&\mathcal{L}_{\mathrm{g}}(C_4\mathrm{e}^{\eta}+C_5\mathrm{e}^{-\eta})=0,\end{aligned} \tag{30}$$

where C_{i} $(i=1-5)$ are arbitrary constants. Denoting $p\in[0,1]$ an embedding parameter and $\hbar_f$, $\hbar_{\mathrm{g}}$ the nonzero auxiliary parameters, we get the following zeroth-order problems:

$$\begin{aligned}&(1-p)\mathcal{L}_{\mathrm{f}}[\widehat{f}(\eta;p)-f_0(\eta)]\\&=p\hbar_{\mathrm{f}}N_{\mathrm{f}}[\widehat{f}(\eta;p),\widehat{g}(\eta;p)],\end{aligned} \tag{31}$$

$$\begin{aligned}&(1-p)\mathcal{L}_{\mathrm{g}}[\widehat{g}(\eta;p)-g_0(\eta)]\\&=p\hbar_{\mathrm{g}}N_{\mathrm{g}}[\widehat{f}(\eta;p),\widehat{g}(\eta;p)],\end{aligned} \tag{32}$$

$$\begin{aligned}&\widehat{f}(0;p)=0, \quad \widehat{f}'(0;p)=1, \quad \widehat{f}'(\infty,p)=0,\\&\widehat{g}(0;p)=0, \quad \widehat{g}(\infty;p)=0,\end{aligned} \tag{33}$$

$$\begin{aligned}&N_{\mathrm{f}}[\widehat{f}(\eta;p),\widehat{g}(\eta;p)]=\frac{\partial^3\widehat{f}(\eta;p)}{\partial\eta^3}\\&-\frac{2n}{n+1}\left(\frac{\partial\widehat{f}(\eta;p)}{\partial\eta}\right)^2+\widehat{f}(\eta;p)\frac{\partial^2\widehat{f}(\eta;p)}{\partial\eta^2}\\&+\frac{4\lambda}{n+1}\widehat{g}(\eta;p)-M^2\frac{\partial\widehat{f}(\eta;p)}{\partial\eta}-\phi\frac{\partial\widehat{f}(\eta;p)}{\partial\eta},\end{aligned} \tag{34}$$

$$\begin{aligned}&N_{\mathrm{g}}[\widehat{f}(\eta;p),\widehat{g}(\eta;p)]=\frac{\partial^2\widehat{g}(\eta;p)}{\partial\eta^2}\\&-\frac{2n}{n+1}\widehat{g}(\eta;p)\frac{\partial\widehat{f}(\eta;p)}{\partial\eta}+\widehat{f}(\eta;p)\frac{\partial\widehat{g}(\eta;p)}{\partial\eta}\\&-\frac{4\lambda}{n+1}\frac{\partial\widehat{f}(\eta;p)}{\partial\eta}-M^2\widehat{g}(\eta;p)-\phi\widehat{g}(\eta;p).\end{aligned} \tag{35}$$

For $p=0$ and $p=1$, one has

$$\begin{aligned}&\widehat{f}(\eta;0)=f_0(\eta), \quad \widehat{g}(\eta;0)=g_0(\eta)\\&\widehat{f}(\eta;1)=f(\eta), \quad \widehat{g}(\eta;1)=g(\eta).\end{aligned} \tag{36}$$

When p increases from 0 to 1, $\widehat{f}(\eta;p)$, $\widehat{g}(\eta;p)$ varies from the initial guesses $f_0(\eta)$, $g_0(\eta)$ to the solutions $f(\eta)$, $g(\eta)$. By Taylor's theorem and (31) and (32) we can write

$$\begin{aligned}\widehat{f}(\eta;p) &= f_0(\eta)+\sum_{m=1}^{\infty} f_{\mathrm{m}}(\eta)p^m,\\ \widehat{g}(\eta;p) &= g_0(\eta)+\sum_{m=1}^{\infty} g_{\mathrm{m}}(\eta)p^m,\end{aligned} \tag{37}$$

$$\begin{aligned}f_{\mathrm{m}}(\eta) &= \frac{1}{m!}\left.\frac{\partial^m \widehat{f}(\eta;p)}{\partial \eta^m}\right|_{p=0},\\ g_{\mathrm{m}}(\eta) &= \frac{1}{m!}\left.\frac{\partial^m \widehat{g}(\eta;p)}{\partial \eta^m}\right|_{p=0},\end{aligned} \tag{38}$$

where the convergence of the series (37) depends upon $\hbar_{\mathrm{f}}$ and $\hbar_{\mathrm{g}}$. We choose $\hbar_{\mathrm{f}}$ and $\hbar_{\mathrm{g}}$ in such a way that the series solutions (37) are convergent at $p=1$, then due to (37) one obtains

$$\begin{aligned}f(\eta) &= f_0(\eta)+\sum_{m=1}^{\infty} f_{\mathrm{m}}(\eta),\\ g(\eta) &= g_0(\eta)+\sum_{m=1}^{\infty} g_{\mathrm{m}}(\eta).\end{aligned} \tag{39}$$

The mth-order deformation problems are

$$\mathcal{L}_{\mathrm{f}}[f_{\mathrm{m}}(\eta)-\chi_{\mathrm{m}} f_{m-1}(\eta)] = \hbar_{\mathrm{f}} R^{\mathrm{f}}_{\mathrm{m}}(\eta), \tag{40}$$

$$\mathcal{L}_{\mathrm{g}}[g_{\mathrm{m}}(\eta)-\chi_{\mathrm{m}} g_{m-1}(\eta)] = \hbar_{\mathrm{g}} R^{\mathrm{g}}_{\mathrm{m}}(\eta), \tag{41}$$

$$\begin{aligned}&f_{\mathrm{m}}(\eta)=0, \quad f'_{\mathrm{m}}(\eta)=0, \quad g_{\mathrm{m}}(\eta)=0,\\ &f'_{\mathrm{m}}(\infty)\to 0 \ \text{ and } \ g_{\mathrm{m}}(\infty)\to 0,\end{aligned} \tag{42}$$

$$\begin{aligned}R^{\mathrm{f}}_{\mathrm{m}}(\eta) &= f'''_{m-1}-\frac{2n}{n+1}\sum_{k=0}^{m-1} f'_{m-1-k}f'_{\mathrm{k}}\\ &+\sum_{k=0}^{m-1} f_{m-1-k}f''_{\mathrm{k}}+\frac{4\lambda}{n+1}g_{m-1}-M^2 f'_{m-1}-\phi f'_{m-1},\end{aligned} \tag{43}$$

$$\begin{aligned}R^{\mathrm{g}}_{\mathrm{m}}(\eta) &= g''_{m-1}-\frac{2n}{n+1}\sum_{k=0}^{m-1} g_{m-1-k}f'_{\mathrm{k}}\\ &+\sum_{k=0}^{m-1} f_{m-1-k}g'_{\mathrm{k}}-\frac{4\lambda}{n+1}f'_{m-1}-M^2 g_{m-1}-\phi g_{m-1},\end{aligned} \tag{44}$$

$$\chi_{\mathrm{m}} = \begin{cases} 0, & m\le 1,\\ 1, & m>1.\end{cases} \tag{45}$$

The above problems up to few order of approximations have been solved by the symbolic computation software *Mathematica*. The series solutions are

$$\begin{aligned}f_{\mathrm{m}}(\eta) &= \sum_{n=0}^{m+1}\sum_{q=0}^{m+1-n} a^q_{m,n}\eta^q\exp(-n\eta),\\ g_{\mathrm{m}}(\eta) &= \sum_{n=0}^{m+1}\sum_{q=0}^{m+1-n} b^q_{m,n}\eta^q\exp(-n\eta),\ m\ge 0.\end{aligned} \tag{46}$$

We can calculate all the coefficients $a^q_{m,n}$ and $b^q_{m,n}$ using only the first few,

$$a^0_{0,0}=1, \quad a^0_{0,1}=-1, \quad b^1_{0,1}=1, \tag{47}$$

given by the initial guess approximations for the solutions $f(\eta)$ and $g(\eta)$ in (28). The corresponding Mth-order approximations of (31) – (33) are

$$\begin{aligned}&f(\eta)=\sum_{m=0}^{\infty} f_{\mathrm{m}}(\eta)=\\ &\lim_{M\to\infty}\left[\sum_{m=0}^{M} a^0_{m,0}+\sum_{n=1}^{M+1}\mathrm{e}^{-n\eta}\left(\sum_{m=n-1}^{M}\sum_{q=0}^{m+1-n} a^q_{m,n}\eta^q\right)\right],\end{aligned} \tag{48}$$

$$\begin{aligned}&g(\eta)=\sum_{m=0}^{\infty} g_{\mathrm{m}}(\eta)=\\ &\lim_{M\to\infty}\left[\sum_{m=0}^{M} b^0_{m,0}+\sum_{n=1}^{M+1}\mathrm{e}^{-n\eta}\left(\sum_{m=n-1}^{M}\sum_{q=0}^{m+1-n} b^q_{m,n}\eta^q\right)\right],\end{aligned} \tag{49}$$

4. Analytical Solution of Temperature $\theta(\eta)$

Case a: Constant surface temperature (*CST*)

For this case the initial guess (θ_0) and operator $\mathcal{L}_\theta$ are defined by

$$\theta_0(\eta)=\exp(-\eta), \tag{50}$$

$$\mathcal{L}_\theta = \theta''-\theta, \tag{51}$$

where

$$\mathcal{L}_\theta(C_6\mathrm{e}^{\eta}+C_7\mathrm{e}^{-\eta})=0 \tag{52}$$

and C_6, C_7 are the arbitrary constants. The zeroth and mth-order problems are given by

$$\begin{aligned}&(1-p)\mathcal{L}_\theta[\widehat{\theta}(\eta;p)-\theta_0(\eta)]\\ &=p\hbar_\theta N_\theta[\widehat{\theta}(\eta;p),\widehat{f}(\eta;p),\widehat{g}(\eta;p)],\end{aligned} \tag{53}$$

$$\widehat{\theta}(0;p)=1, \quad \widehat{\theta}(\infty;p)=0, \tag{54}$$

$$\begin{aligned}&N_\theta[\widehat{\theta}(\eta;p),\widehat{f}(\eta;p),\widehat{g}(\eta;p)]=\\ &(3R_{\mathrm{d}}+4)\frac{\partial^2\widehat{\theta}(\eta;p)}{\partial\eta^2}+3R_{\mathrm{d}}\Pr\widehat{f}(\eta;p)\frac{\partial\widehat{\theta}(\eta;p)}{\partial\eta}\\ &+3R_{\mathrm{d}}\Pr\mathrm{Ec}\left[\left\{\frac{\partial^2\widehat{f}(\eta;p)}{\partial\eta^2}\right\}^2+\left\{\frac{\partial\widehat{g}(\eta;p)}{\partial\eta}\right\}^2\right],\end{aligned} \tag{55}$$

$$\mathcal{L}_\theta[\theta_{\rm m}(\eta)-\chi_{\rm m}\theta_{m-1}(\eta)]=\hbar_\theta R^\theta_{\rm m}(\eta), \tag{56}$$

$$\theta_{\rm m}(0)=0,\ \theta_{\rm m}(\infty)\to 0, \tag{57}$$

$$R^\theta_{\rm m}(\eta)=(3R_{\rm d}+4)\theta''_{m-1}(\eta)+3R_{\rm d}\,{\rm Pr}\cdot\left[\theta'_{m-1-k}f_{\rm k}+{\rm Ec}\{f''_{m-1-k}f''_{\rm k}+g'_{m-1-k}g'_{\rm k}\}\right]. \tag{58}$$

The mth-order problem has the solution of the form

$$\theta_{\rm m}(\eta)=\sum_{n=0}^{m+1}\sum_{q=0}^{m+1-n}c^q_{m,n}\eta^q\exp(-n\eta),\quad m\geq 0, \tag{59}$$

where we can calculate all the coefficients $c^q_{m,n}$ using only the first few:

$$c^0_{0,0}=c^1_{0,0}=0,\quad c^0_{0,1}=1. \tag{60}$$

The temperature field is of the form

$$\theta(\eta)=\sum_{m=0}^{\infty}\theta_{\rm m}(\eta)=\lim_{M\to\infty}\left[\sum_{m=0}^{M}c^0_{m,0}+\sum_{n=1}^{M+1}{\rm e}^{-n\eta}\left(\sum_{m=n-1}^{M}\sum_{q=0}^{m+1-n}c^q_{m,n}\eta^q\right)\right]. \tag{61}$$

Case b: Prescribed surface temperature (*PST*)

Employing the same methodology as in case (*a*), the solution here is

$$\theta(\eta)=\sum_{m=0}^{\infty}\theta_{\rm m}(\eta)=\lim_{M\to\infty}\left[\sum_{m=0}^{M}d^0_{m,0}+\sum_{n=1}^{M+1}{\rm e}^{-n\eta}\left(\sum_{m=n-1}^{M}\sum_{q=0}^{m+1-n}d^q_{m,n}\eta^q\right)\right]. \tag{62}$$

5. Convergence of the Analytical Solution

The explicit analytical solutions in (48), (49), (61), and (62) involve $\hbar_{\rm f}$, $\hbar_{\rm g}$, and $\hbar_\theta$ which give the convergence region and rate of approximation for the HAM solution. The $\hbar$-curves are plotted for the 15th-order of approximations for the dimensionless velocity components f', g, and temperature θ in Figure 1. We note that the respective range of admissible values of $\hbar_{\rm f}$, $\hbar_{\rm g}$, and $\hbar_\theta$ is $-0.83\leq\hbar_{\rm f}\leq-0.1$, $-0.75\leq\hbar_{\rm g}\leq-0.3$, and $-0.45\leq\hbar_\theta\leq-0.05$.

6. Results and Discussion

This section illustrates the effect of varying some interesting parameters on the velocity and temperature

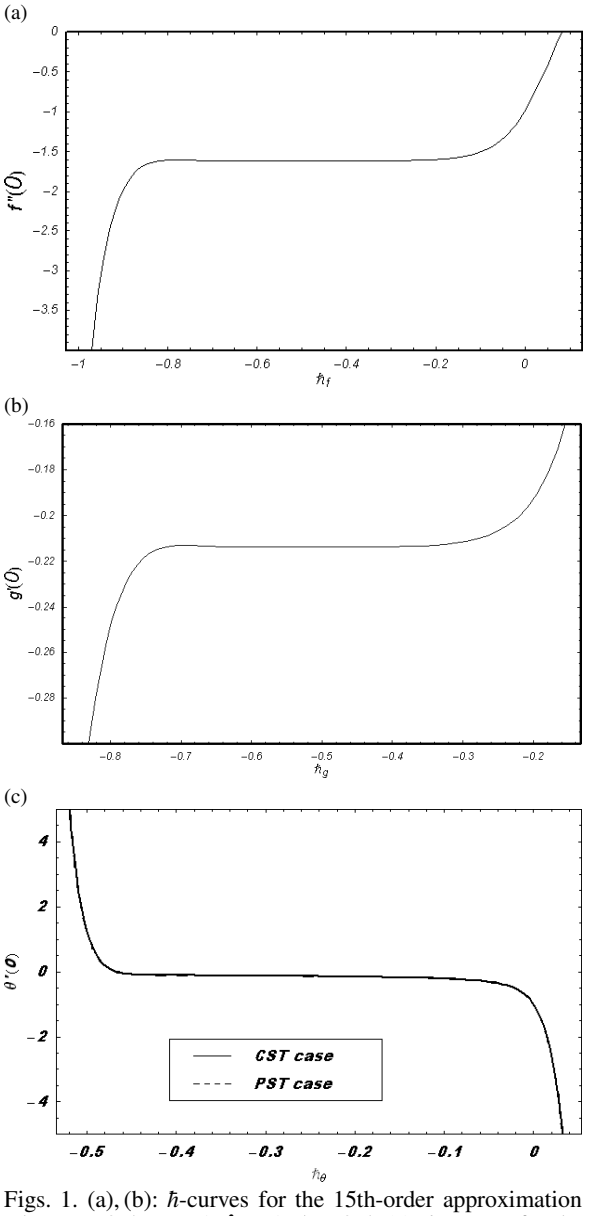

Figs. 1. (a), (b): $\hbar$-curves for the 15th-order approximation when $n=0.5$, $M=1$, $\lambda=1$, $\phi=0.5$; (c): $\hbar_\theta$-curve for the 15th-order approximation when $n=0.5$, $M=0.1$, $\lambda=0.1$, $\phi=0.5$, ${\rm Pr}=0.5$, $R_{\rm d}=0.1$, ${\rm Ec}=\tilde{\rm E}{\rm c}=0.1$.

profiles. For that Figures 2 – 12 have been sketched. To be more specific, attention has been given to the variations of n, the Hartman number M, rotation parameter λ, porosity parameter ϕ, Prandtl number Pr, radiation parameter $R_{\rm d}$, and Eckert numbers Ec and $\tilde{\rm E}{\rm c}$ on the velocity and temperature fields, respectively. In order to see the effects of n, the Hartman number M, the rotation parameter λ, and the porosity parameter ϕ

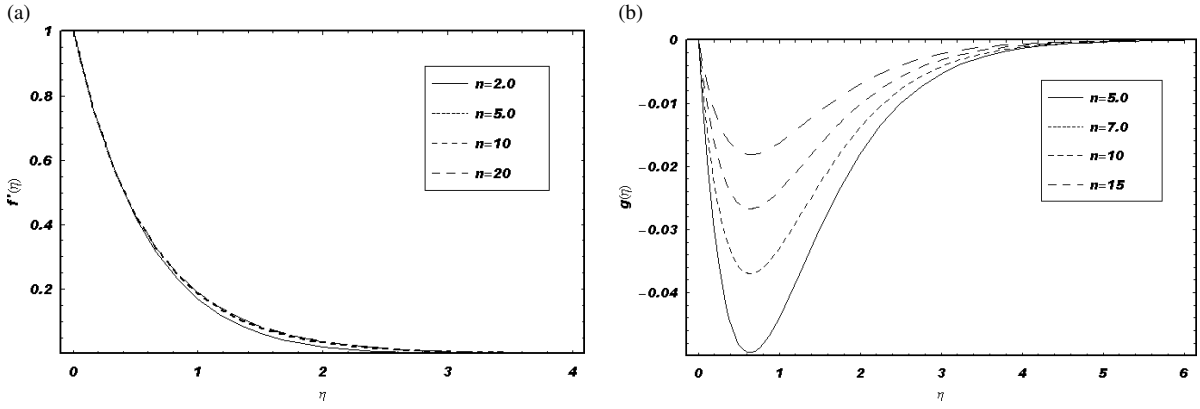

Figs. 2. Effects of n on f' and g when $M = 1$, $\lambda = 1$, $\phi = 0.5$, $\hbar_f = \hbar_g = -0.3$.

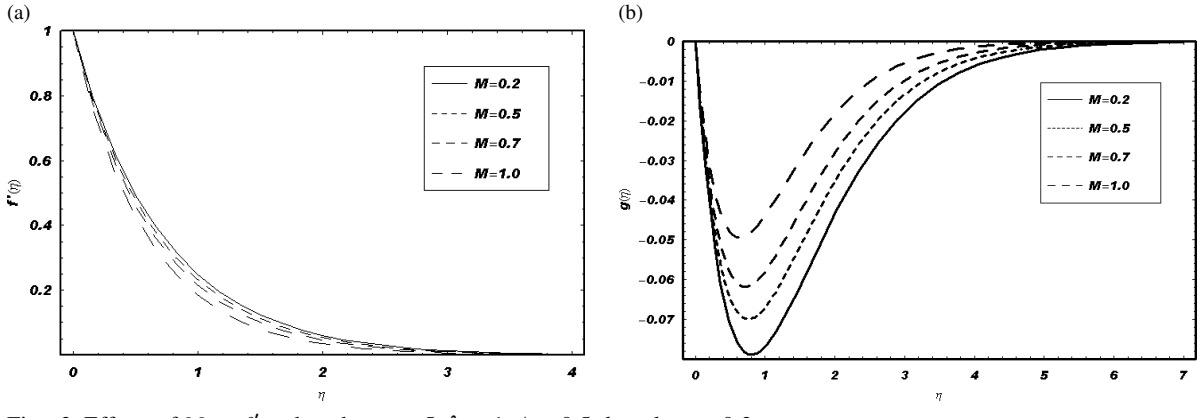

Figs. 3. Effects of M on f' and g when $n = 5$, $\lambda = 1$, $\phi = 0.5$, $\hbar_f = \hbar_g = -0.3$.

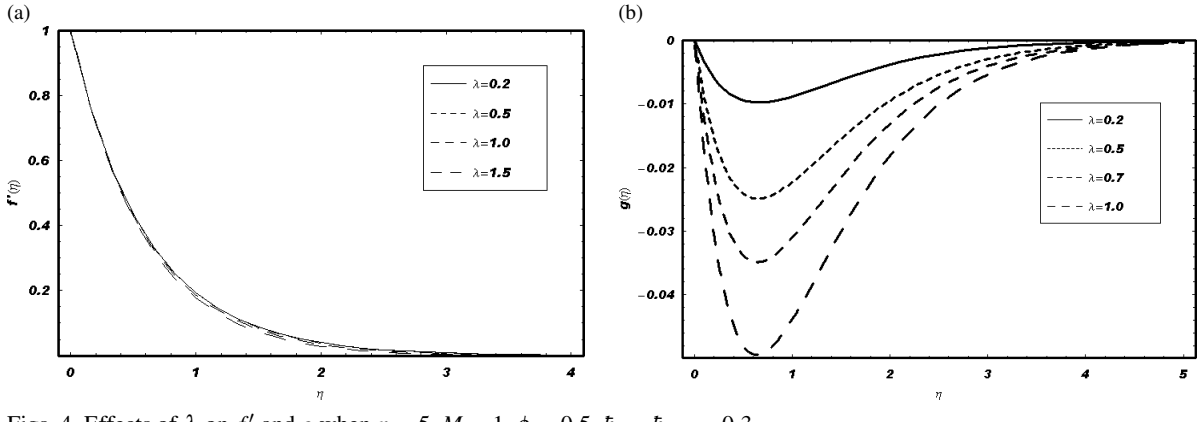

Figs. 4. Effects of λ on f' and g when $n = 5$, $M = 1$, $\phi = 0.5$, $\hbar_f = \hbar_g = -0.3$.

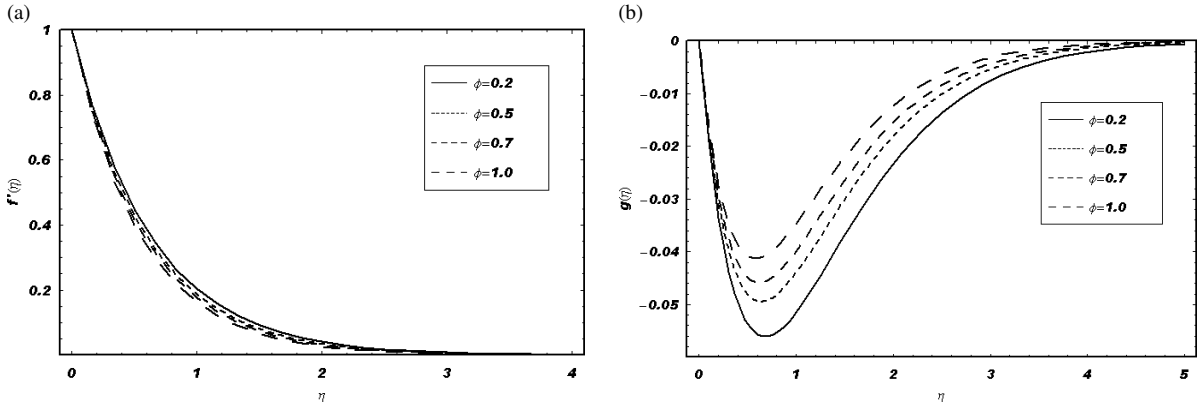

Fig. 5. Effects of ϕ on f' and g when $n = 5$, $M = 1$, $\lambda = 1$, $\hbar_{\rm f} = \hbar_{\rm g} = -0.3$.

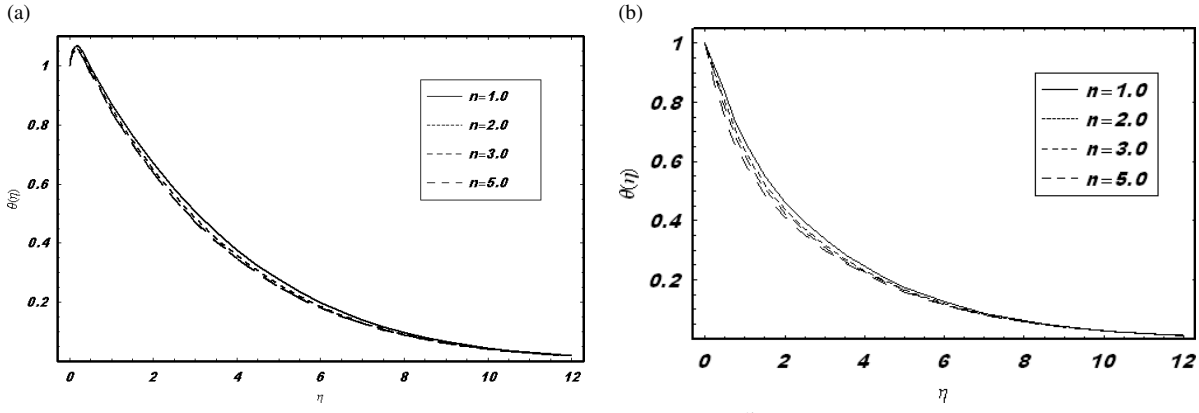

Fig. 6. Effects of n on θ when $\Pr = 1$, $R_{\rm d} = 1$, $M = 1$, $\phi = 0.5$, $\mathrm{Ec} = 1$, $\tilde{\mathrm{E}}\mathrm{c} = 0.5$, $\hbar_\theta = -0.3$ for CST and PST cases, respectively. Here $\lambda = 1$ in (a) and $\lambda = 0.2$ in (b).

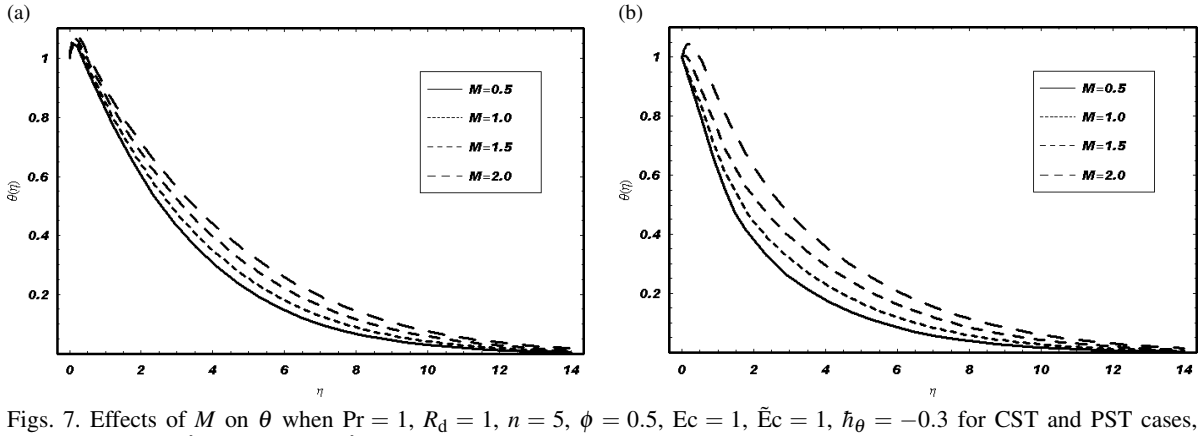

Figs. 7. Effects of M on θ when $\Pr = 1$, $R_{\rm d} = 1$, $n = 5$, $\phi = 0.5$, $\mathrm{Ec} = 1$, $\tilde{\mathrm{E}}\mathrm{c} = 1$, $\hbar_\theta = -0.3$ for CST and PST cases, respectively. Here $\lambda = 1$ in (a) and $\lambda = 0.5$ in (b).

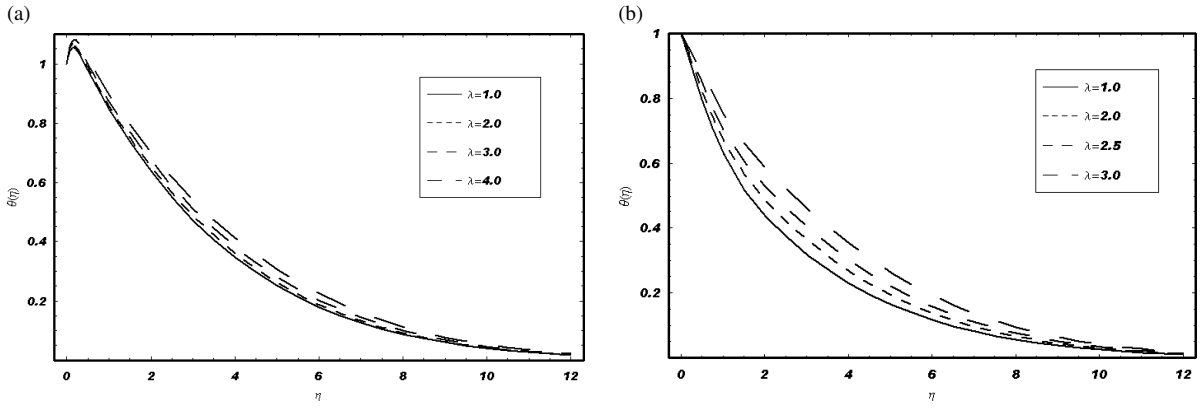

Figs. 8. Effects of λ on θ when $\mathrm{Pr} = 1$, $R_{\mathrm{d}} = 1$, $M = 1$, $\phi = 0.5$, $\mathrm{Ec} = 1$, $\tilde{\mathrm{E}}\mathrm{c} = 0.5$, $\hbar_\theta = -0.3$ for CST and PST cases, respectively. Here $n = 5$ in (a) and $n = 3$ in (b).

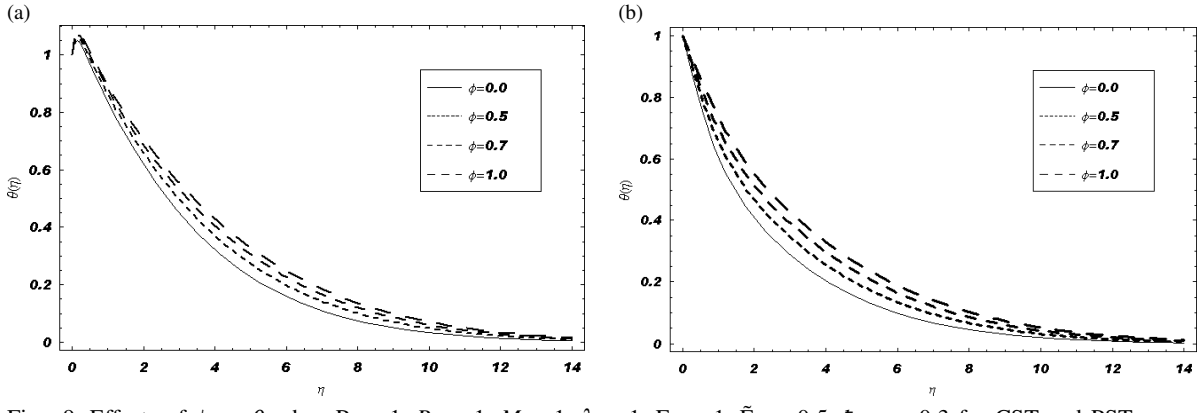

Figs. 9. Effects of ϕ on θ when $\mathrm{Pr} = 1$, $R_{\mathrm{d}} = 1$, $M = 1$, $\lambda = 1$, $\mathrm{Ec} = 1$, $\tilde{\mathrm{E}}\mathrm{c} = 0.5$, $\hbar_\theta = -0.3$ for CST and PST cases, respectively. Here $n = 5$ in (a) and $n = 3$ in (b).

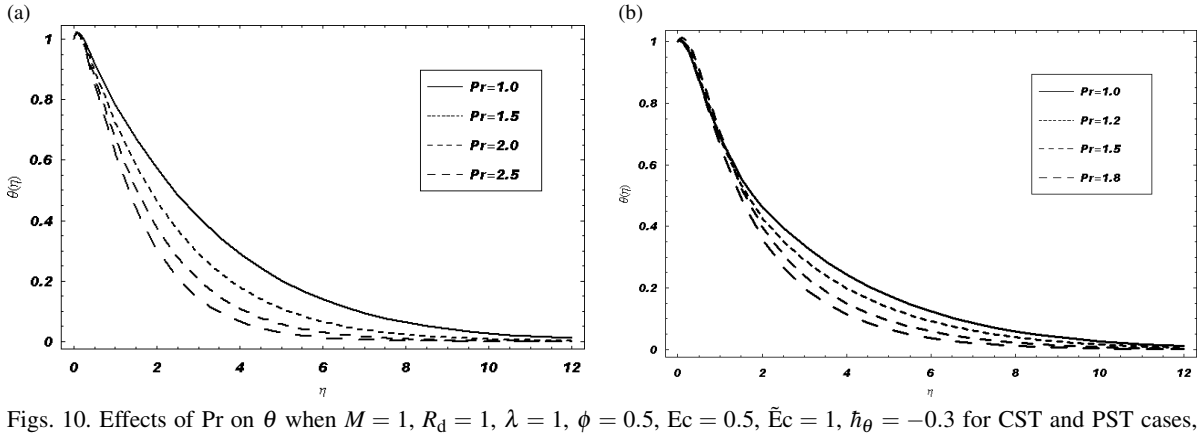

Figs. 10. Effects of Pr on θ when $M = 1$, $R_{\mathrm{d}} = 1$, $\lambda = 1$, $\phi = 0.5$, $\mathrm{Ec} = 0.5$, $\tilde{\mathrm{E}}\mathrm{c} = 1$, $\hbar_\theta = -0.3$ for CST and PST cases, respectively. Here $n = 5$ in (a) and $n = 3$ in (b).

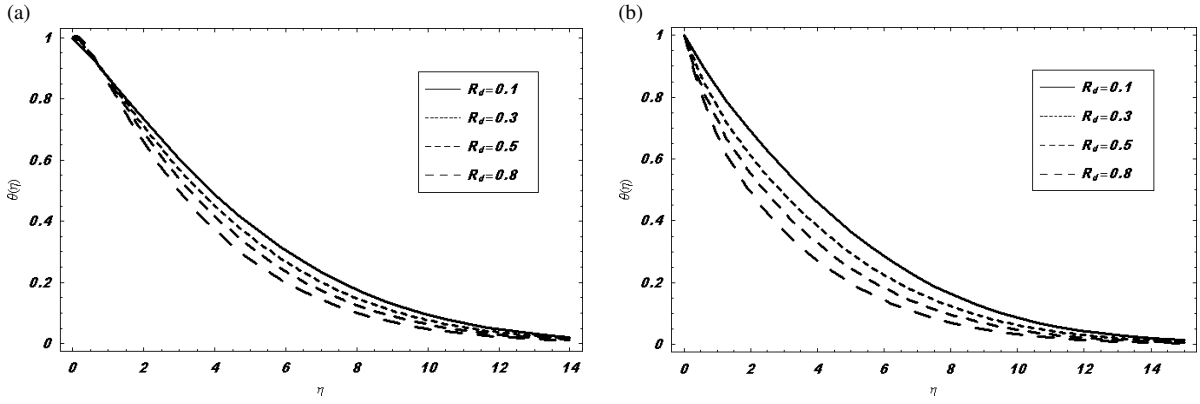

Figs. 11. Effects of $R_{\rm d}$ on θ when $\Pr = 1$, $M = 1$, $\lambda = 1$, $\phi = 0.5$, $\mathrm{Ec} = 1$, $\tilde{\mathrm{E}}\mathrm{c} = 1$, $\hbar_\theta = -0.3$ for CST and PST cases, respectively. Here $n = 5$ in (a) and $n = 3$ in (b).

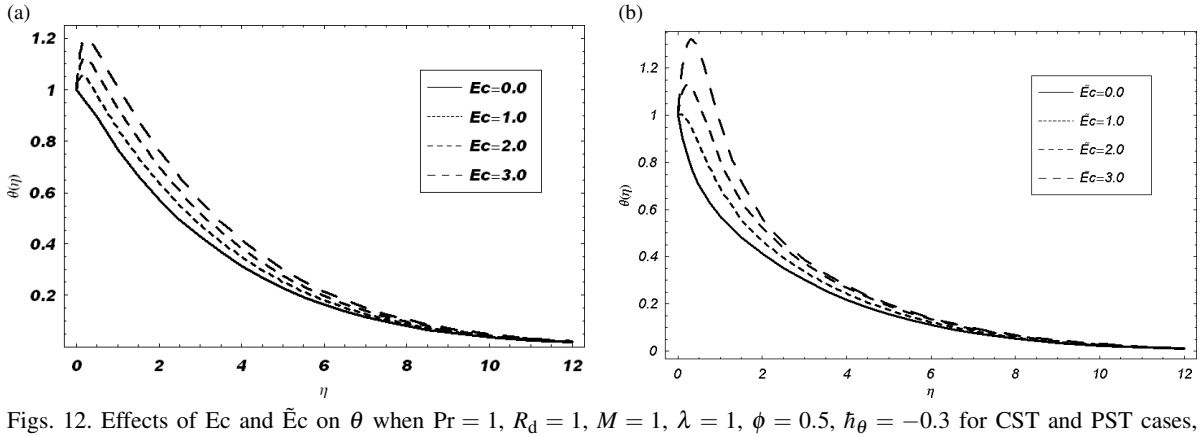

Figs. 12. Effects of Ec and $\tilde{\mathrm{E}}\mathrm{c}$ on θ when $\Pr = 1$, $R_{\rm d} = 1$, $M = 1$, $\lambda = 1$, $\phi = 0.5$, $\hbar_\theta = -0.3$ for CST and PST cases, respectively. Here $n = 5$ in (a) and $n = 3$ in (b).

on the velocity components f' and g, we prepared Figures 2 – 5. Figure 2 shows that there is a small change in f' by increasing n. However, there is a significant change when n is changed and M, λ, and ϕ are fixed. This figure indicates that the magnitude of g increases by increasing n. The effect of the magnetic force M on the flow velocity f' and g are shown in Figure 3. The effect of M on f' and g is significant here. We conclude that an increase in M leads to the decrease in f' and increase in g. The variation of λ on $f'$and g is shown in Figure 4. This figure shows that f' decreases. The behaviour of λ on the magnitude of g is quite opposite of f'. Figure 5 depicts the effects of the porosity parameter ϕ on f' and g. It is found that the effect of the porosity parameter on f' and g is similar to that of the Hartman number M.

Figures 6a – 12a show the behaviour of various parameters on the temperature profile for the CST case. Figure 6a indicates that θ decreases for large values of n. Figures 7a and 8a depict that the temperature distribution increases when M and λ increases. Figure 9a illustrates the variation of porosity parameter ϕ on the temperature θ. It is found that θ increases as ϕ increases. The effect of varying the Prandtl number on the temperature profile is sketched in Figure 10a. Here θ decreases as Pr increases. The influence of the radiation parameter $R_{\rm d}$ on θ is shown in Figure 11a. It can be seen that an increase in $R_{\rm d}$ parameter leads to a decrease in θ. The influence of the Eckert number Ec on temperature field is illustrated in Figure 12a. It describes that θ is an increasing function of Ec.

Figures 6b – 12b are plotted to see the effects of the above mentioned parameters on the temperature profile for PST case. Figure 6b depicts the effect of n on θ. It is noted that this figure shows the similar results when compared with Figure 6a. Figure 7b has the same behaviour as compared to the CST case. However, the increment is large compared with the CST case. Fig-

sures 8b and 9b show an increase in temperature as the rotation and porosity parameter increases. But this increment is large compared with the CST case. Figure 10b displays the same behaviour as in the CST case. However, this decrement is small compared with Figure 10a. Figures 11b and 12b have the same results as in the CST case.

7. Concluding Remarks

In this paper, we have sought to determine how the effects of radiation on MHD rotating flow of a viscous fluid over a nonlinear stretching sheet are analyzed. The series solutions for the velocity and temperature fields are developed using HAM. The role of some various emerging parameters on the velocity components and temperature is shown and discussed properly. The following observations are made from the above analysis:

- The velocity f' increases by increasing n.
- The velocity g increases for large values of n, M, and ϕ.
- The temperature θ increases for large values of M, λ, ϕ, Ec, and $\tilde{\text{E}}$c.
- The temperature θ decreases as n, Pr, and R_{d} increases.

[1] S. J. Liao, Ph.D Thesis, Shanghai Jiao Tong University 1992.
[2] S. J. Liao, Beyond perturbation: Introduction to homotopy analysis method, Chapman & Hall/CRC Press, Boca Raton 2003.
[3] S. J. Liao, Nonlinear Anal.: Real World Appl. **10**, 2455 (2009).
[4] S. J. Liao, Commun. Nonlinear Sci. Numer. Simul. **14**, 983 (2009).
[5] S. J. Liao, Appl. Math. Comput. **169**, 1186 (2005).
[6] S. Abbasbandy, Chaos, Solitons, and Fractals **36**, 581 (2008).
[7] S. Abbasbandy, Chem. Eng. J. **136**, 144 (2008).
[8] S. Abbasbandy, Int. J. Heat Mass Transf. **34**, 380 (2007).
[9] S. Abbasbandy, Nonlinear Dyn. **52**, 35 (2008).
[10] F. M. Allan, Appl. Math. Comput. **190**, 6 (2007).
[11] M. Inc, Phys. Lett. A **21**, 356 (2008).
[12] T. Hayat, M. Sajid, and I. Pop, Nonlinear Anal.: Real World Appl. **9**, 1811 (2008).
[13] M. Sajid and T. Hayat, Chaos, Solitons, and Fractals **38**, 506 (2008).
[14] T. Hayat, T. Javed, and Z. Abbas, Nonlinear Anal. B **10**, 1514 (2009).
[15] T. Hayat, T. Javed, and M. Sajid, Phys. Lett. A **372**, 3264 (2008).
[16] T. Hayat, Z. Abbas, and M. Sajid, Phys. Lett. A **372**, 2400 (2008).
[17] M. Sajid and T. Hayat, Int. Commun. Heat Mass Transf. **35**, 347 (2008).
[18] T. Hayat, Z. Abbas, and T. Javed, Phys. Lett. A **372**, 637 (2008).
[19] M. Sajid and T. Hayat, Chaos, Solitons, and Fractals **39,** 1317 (2009).
[20] M. Sajid and T. Hayat, Phys. Lett. A **372**, 1827 (2008).
[21] A. R. Bestman and S. K. Adjepong, Astrophys. Space Sci. **143**, 73 (1988).
[22] H. S. Takhar, R. Gorla, and V. M. Soundalgekar, Int. J. Numer. Methods Heat Fluid Flow **6**, 77 (1996).
[23] A. Raptis, C. Perdikis, and H. S. Takhar, Appl. Math. Comput. **153**, 645 (2004).